

Thermodynamics phase changes of nanopore fluids



Akand W. Islam^{a,*}, Tad W. Patzek^b, Alexander Y. Sun^a

^a Bureau of Economic Geology, University of Texas at Austin, Austin, TX, USA

^b Earth Science and Engineering Division, King Abdullah University of Science & Technology, Thuwal, Saudi Arabia

ARTICLE INFO

Article history:

Received 16 January 2015

Received in revised form

26 April 2015

Accepted 27 April 2015

Available online 15 May 2015

Keywords:

Phase change

Confined fluid

Nanopore

van der Waals equation

Critical shift

ABSTRACT

The van der Waals (vdW) equation (Eq.) is modified to describe thermodynamic of phase behavior of fluids confined in nanopore. Our aim is to compute pressures exerted by the fluid molecules and to investigate how they change due to pore proximity by assuming the pore wall is inert. No additional scaling of model parameters is imposed and original volume and energy parameters are used in the calculations. Our results clearly show the phase changes due to confinement. The critical shifts of temperatures and pressures are in good agreement compared to the laboratory data and molecular simulation. Peng–Robinson (PR) equation-of-state (EOS) has resulted in different effect than the vdW. This work delivers insights into the nature of fluid behavior in extremely low-permeability nanoporous media, especially in the tight shale reservoirs, below the critical temperatures.

© 2015 Elsevier B.V. All rights reserved.

1. Introduction

The phase behavior of fluids confined in porous media is an important subject of many practical applications, such as separation processes, oil extraction, estimation of gas-in-place and reserves, heterogeneous catalysis, molecular transport, among others (Holt et al., 2006; Travalloni et al., 2010a; Didar and Akkutlu, 2013). The energy dissipated by the friction due to confinement induces liquid–gas phase transitions, chemical transformations, and also drastic changes of static and dynamic properties, such as shear stress, compressibility, coefficient of friction, and viscosity (Zarragoicochea and Kuz, 2002). The dynamic and static property changes are different from bulk behavior even qualitatively (Singer and Pollock, 1992). The confinement effect becomes important as the dimensions of the pores shrink. Fluids confined within pores of nanometer are in between bulk matters and single atoms or molecules and, as a consequence, finite size and surface effects must be investigated (Singh et al., 2009). Any real system interfaces either with walls of a container, or with different phases of the substance under consideration. Fluids trapped in pore spaces with the dimensions of 5–10 molecules organize as layers, and within each layer lateral order exists. A particular structure exists across thin films and an oscillatory force decaying exponentially varies

between attraction and repulsion with a periodicity of the scale of molecular dimension (Zarragoicochea and Kuz, 2002; McGuiggan and Israelachvili, 1990; Varnik et al., 2000). Pot et al. (1996) presented a lattice-gas cellular automata porous media model exhibiting vapor–liquid equilibrium of microscopic fluid on solid walls. Their study implicitly revealed a fluid in nanopore experiences tensorial effect. Thermodynamic model should describe this phenomenon. There are few laboratory experiments conducted to study the confinement at nanopore scale (Morishige et al., 1997; Morishige and Shikimi, 1998; Konno et al., 1985; Sakuth et al., 1998; Yun et al., 2004). Imaging tools although powerful are unable to provide us with an understanding of the underlying mechanisms of how fluids reside and flow in nanopores (Didar and Akkutlu, 2013). This shortcoming necessitates the employment of theoretical methods such as molecular simulation (Didar and Akkutlu, 2013; Singh et al., 2009; Coasne et al., 2009; Demontis et al., 2003; Dukovski et al., 2000; Giovambattista et al., 2009; Jiang and Sandler, 2006; Nicholson and Parsonage, 1982; Severson and Snurr, 2007; Diaz-Campos, 2010; Jiang et al., 2005; Jiang and Sandler, 2005; Binder et al., 2003) and density functional theories (Kotdawala et al., 2005; Travalloni et al., 2010b; Wu, 2006). However these tools are computationally expensive. Studying distributions of fluid mixtures in a large-scale heterogeneous porous matrix is not possible by using these schemes. Hence researchers (Zarragoicochea and Kuz, 2002; Schoen and Diestler, 1998; Giaya and Thompson, 2002; Meyra et al., 2005; Derouane, 2007; Vakili-Nezhaad and Mansoori, 2006) have focused on developing

* Corresponding author.

E-mail address: Akand.Islam@beg.utexas.edu (A.W. Islam).

Notations

A	pore cross sectional area [dm ²]
a	vdW energy parameter [Padm ⁶ mol ⁻²]
b	vdW volume parameter [dm ³ mol ⁻¹]
d_p	pore diameter [dm]
F	Helmholtz free energy [kg dm ² s ⁻²]
k	Boltzman constant
L	length [dm]
N	Avogadro number
P	pressure [MPa]
r_p	pore radius [dm]
s	inter molecular distance [dm]
R	universal gas constant [dm ³ MPa mol ⁻¹ K ⁻¹]
T	temperature [K]
v	specific volume [dm ³ mol ⁻¹]
V	pore volume [dm ³]

Greek symbol

σ	Lennard-Jones size parameter
ϵ	Lennard-Jones energy parameter

Subscripts

1,2	molecules id's
B	bulk
p	pore
red	reduced

Superscript

c	critical
-----	----------

Axes

x	axial direction
r	radial direction

analytical (semi empirical) EOS models. To study small systems one needs to modify the basic equations of the conventional (bulk) thermodynamics. The fundamental concept of phase equilibrium of nano systems was first introduced by Hill (2002) in early sixties. However there are still serious challenges in defining the environmental variables in nano systems, such as temperature and pressure. Parallel to thermodynamics of nano systems many attempts have been made by using the concept of non-extensive statistical mechanics and thermodynamics (Vakili-Nezhaad and Mansoori, 2006). Tsallis (1988, 1999) showed close relation between nanothermodynamics and non-extensive thermodynamics through the fundamental parameters (Vakili-Nezhaad and Mansoori, 2004). In this article we focus on an EOS to address the nano confinement effects (i.e., the pore size effect). The equation describes the fluid behavior from the bulk state to extreme confinement.

Extensions of the vdW EOS to confined fluids have been studied to predict the critical temperature change with pore size both qualitatively and quantitatively. Schoen and Diestler (1998) showed application of vdW to model fluids confined in slit pores based on perturbation theory. The capillary condensation and reduction in the critical temperature of the fluid due to confinement were predicted. The performance of the model near the critical point of bulk fluid was not satisfactorily. The assumption of a universal reference fluid could be the cause as observed by Travalloni et al. (2010b). Giaya and Thompson (2002) obtained good predictions of water adsorption on two different mesoporous formations. To study the phase behavior of confined fluids Zarragoicoechea and Kuz (2002) have improved the vdW considering the tensorial nature of pressure in nanopores. Their work was based on classical thermodynamics and aimed to understand fluids pressure tensor change due to pore size reduction. Therefore the pore-wall interaction was ignored. The capillary condensation measured was consistent with molecular simulation. However, the scaling relations are not good enough to show transition from a confined to bulk critical property. For instance, the critical temperature of bulk phase ($\sigma/r_p \rightarrow 10^{-5}$) CH₄ calculated is 113 K where the true value is 191 K. In a followed-up article (Zarragoicoechea and Kuz, 2004) they improved their model by regressing original energy and volume parameters of vdW. Here we show that even with no additional scaling of model parameters the vdW can be applied to confined fluids in nanopore. Our objective is to demonstrate the critical shifts both qualitatively and quantitatively. In addition,

comparison with another classical EOS, such as PR, is shown. A thorough literature survey (Didar and Akkutlu, 2013; Singh et al., 2009; Morishige et al., 1997; Morishige and Shikimi, 1998; Zarragoicoechea and Kuz, 2004; Vishnyakov et al., 2001; Ortiz et al., 2005; Jana et al., 2009; Devegowda et al., 2012) is performed to collect the critical shifts obtained from experiments and molecular simulation.

Other investigations on this subject include Vakili-Nezhaad and Mansoori (2006), who used the exact form of Zarragoicoechea and Kuz (2002) equation to interpret phase change or fragmentation. Derouane (2007) proposed a simple modification of the attractive part of vdW to apply for fluids in microporous solids far from saturation. Travalloni et al. (2010b) extended vdW to describe different types of adsorption isotherms. Later Travalloni et al. (2010a) presented critical behavior of pure confined fluids. The effects of pore size and intensity of the molecule–wall interaction were evaluated. However their new molecule–wall interaction term in the model equation is hypothetical and no suggestion is proposed for any particular pore wall structure.

2. Model

Here we show the model development. Pressure \vec{P} is a diagonal tensor expressed as $\vec{P}(p_i, i = x, r)$. The pore model is shown in Fig. 1. The Helmholtz free energy of N particles interacting by a pair potential $U(s_{12})$ can be read as

$$F = f(T) - \frac{kTN^2}{2V^2} \iint \left(e^{-\frac{U(s_{12})}{kT}} - 1 \right) dV_1 dV_2. \quad (1)$$

Here $f(T)$ is the free energy of ideal gas. Because we are interested in measuring the pressure force exerted by the fluid molecules the pore wall is assumed to be non-wetting. For Lennard-Jones potential $U(s_{12})$ equals $4\epsilon[(\sigma/s_{12})^{12} - (\sigma/s_{12})^6]$. By following the derivations shown by Zarragoicoechea and Kuz (2002) a form of F becomes

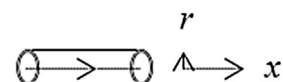


Fig. 1. Schematic diagram of pore model.

$$F = f(T) + \frac{kTN^2}{V}b + \frac{kTN^2}{2V^2} \int_{s_{12} > \sigma} \int U(s_{12}) \frac{dV_1 dV_2}{kT} \quad (2)$$

By assuming $s_{12} > \sigma$, we solve the double integral numerically as

$$\frac{1}{V} \iint_{s_{12} > \sigma} \frac{U(s_{12})}{kT} dV_1 dV_2 = \frac{4\epsilon}{kT} \sigma^3 f\left(\frac{d_p}{\sigma}\right). \quad (3)$$

Here $f(d_p/\sigma) = \left[c_0 + c_1/d_p/\sigma + c_2/\left(\frac{d_p}{\sigma}\right)^2 \right]$. From data regressions we obtain $c_0 = -2.7925$, $c_1 = 2.6275$, and $c_2 = -0.6743$. The numerical values of Eq. (3) and of $f(d_p/\sigma)$ are shown in Fig. 2. The cylindrical pore volume and the specific molar volume are $V = A_p L_x = \pi r_p^2 L_x$ and $v = \frac{V}{N} \Big|_{N \rightarrow \infty}$, respectively.

Differentiating the Helmholtz free energy by the relation of $P_r = -\frac{\sigma^2}{L_x} \frac{\partial F}{\partial A_p} \Big|_{T, L_x}$, $P_x = -\frac{\sigma^2}{A_p} \frac{\partial F}{\partial L_x} \Big|_{T, A_p}$, and letting $c_0 = -a/2\epsilon\sigma^3$ we obtain the radial pressure as

$$P_r = \frac{RT}{v-b} - \frac{a - \sigma^3 \epsilon N^2 \frac{\sigma}{r_p} \left(3c_1 + 4c_2 \frac{\sigma}{r_p} \right)}{v^2}. \quad (4)$$

The axial pressure is deduced as

$$P_x = \frac{RT}{v-b} - \frac{a - 2\sigma^3 \epsilon N^2 \frac{\sigma}{r_p} \left(c_1 + c_2 \frac{\sigma}{r_p} \right)}{v^2}. \quad (5)$$

The Eqs. (4) and (5) preserve the original vdW constants, a and b . For $\sigma/r_p \rightarrow 0$ the equations reduce to the original vdW form. The critical temperature, pressure, and volume are deduced by solving following differential equations

$$\frac{\partial P_x}{\partial v} \Big|_T = \frac{\partial^2 P_x}{\partial v^2} \Big|_T = 0 \quad (6)$$

The critical terms obtained are

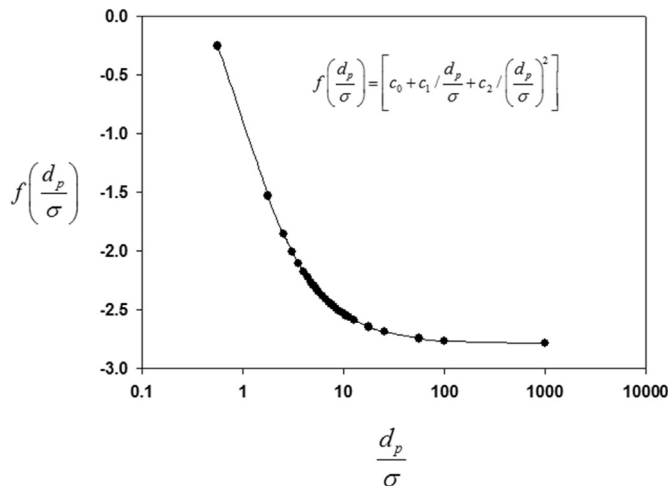


Fig. 2. Curve fitting of $f(d_p/\sigma)$ (The circles represent numeric values of double integral of Eq. (3) and the line shows the quadratic fit using Eq. (3)).

$$T_c = \frac{8}{27bR} \left[a - 2\sigma^3 \epsilon N^2 \frac{\sigma}{r_p} \left(c_1 + c_2 \frac{\sigma}{r_p} \right) \right],$$

$$P_c = \frac{1}{27b^2} \left[a - 2\sigma^3 \epsilon N^2 \frac{\sigma}{r_p} \left(c_1 + c_2 \frac{\sigma}{r_p} \right) \right], \quad \text{and } v_c = 3b.$$

3. Results and discussion

Eqs. (4) and (5) compute the radial and axial components of the pressure tensor of confined fluid in term of σ/r_p in a cylindrical pore of infinite length ($L_x \rightarrow \infty$). Fig. 3 shows the P - v diagrams at constant reduced temperature ($T_{red} = T/T_B^c$) and pore sizes for CH_4 and N_2 . The model equations show that the axial pressure is lower than the radial. Actually when the temperature is subcritical, Maxwell construction appears to balance the axial pressure. The vapor–liquid equilibrium (VLE) or capillary condensation occurs in the vicinity of pore wall. The homogeneous gas phase separates from the liquid. The fluid's global or effective pressure is assumed as $P_{eff} = 1/2(P_x + P_r)$. P_{eff} clearly shows the Maxwell loop revealing the existence of VLE. From this tie line the equilibrium vapor and liquid densities can also be predicted. Although the wall–molecules interaction is not considered capillary condensation exists. The results are critically important for accurate forecast of shale gas

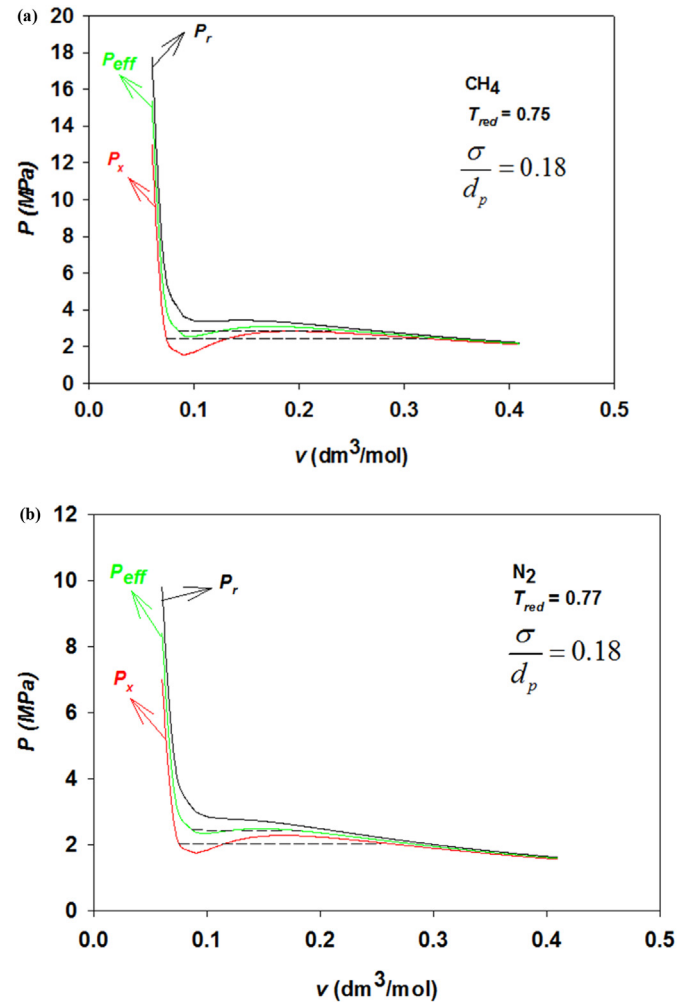


Fig. 3. P - v diagram calculated from proposed Eqs. (4) and (5). Dots represent Maxwell's construction relating to vapor–liquid equilibrium.

productions where the permeability of tight reservoirs can be in nanoscales. These explain reasons for the significant production of condensate liquids from the nanoporous media in contrast to what is expected based on the industry's collective experience with conventional reservoirs (Didar and Akkutlu, 2013; Devegowda et al., 2012).

We have attempted to reproduce the critical shifts with our proposed model. The results are shown in Fig. 4. Here $\Delta T^c = T_B^c - T_p^c/T_B^c$. The shifts of critical temperatures of O₂, Ar, Xe, CO₂, C₂H₄, and N₂ are collected from Morishige et al. (1997), Morishige and Shikimi (1998), Zarragoicoechea and Kuz (2004); CH₄ from Didar and Akkutlu (2013), Singh et al. (2009), Vishnyakov et al. (2001), Ortiz et al. (2005), Devegowda et al. (2012); and C₄H₁₀ from Singh et al. (2009). As pore size decreases the critical temperature reduces almost linearly. Our proposed model can capture the reductions quite well especially up to the limit when pore size is twice the hard sphere molecules ($\sigma/d_p \approx 0.5$). The deviations arise due to omitting the different degrees of multilayer adsorption preceding the capillary condensations. The pore wall is assumed to be inert. Our simple model also quantifies the critical pressure shifts ($\Delta P^c = P_B^c - P_p^c/P_B^c$) shown in Fig. 5. Calculations are compared with molecular simulation of CH₄ (Didar and Akkutlu, 2013; Devegowda et al., 2012), C₄H₁₀ (Singh et al., 2009), and C₈H₁₈ (Singh et al., 2009). Negative pressure shifts are discarded (Singh et al., 2009; Devegowda et al., 2012). Results are deviated mainly because of neglecting surface tension effects. From Figs. 4 and 5 we can reveal that the critical pressure is more sensitive to pore proximity than the critical temperature. This is supported by Singh et al. (2009). They have showed some cases where the shifts can be even negative, i.e., $P_p^c > P_B^c$ based on different material wall properties. Because we have assumed inert pore the negative shifts could not be modeled by the vdW presented. Unlike the case of critical temperatures critical pressure shifts data are scant. This certainly warrants more investigations. The critical temperatures and pressures, Lennard-Jones potential parameters, values of vdW energy and volume terms used in calculations are obtained from Smith et al. (2005), Hirschfelder et al. (1993), and Weast (1972), respectively.

We have applied PR (Peng and Robinson, 1976) empirical relation of $v(v+b) + b(v-b)$ in attraction term and recalculated

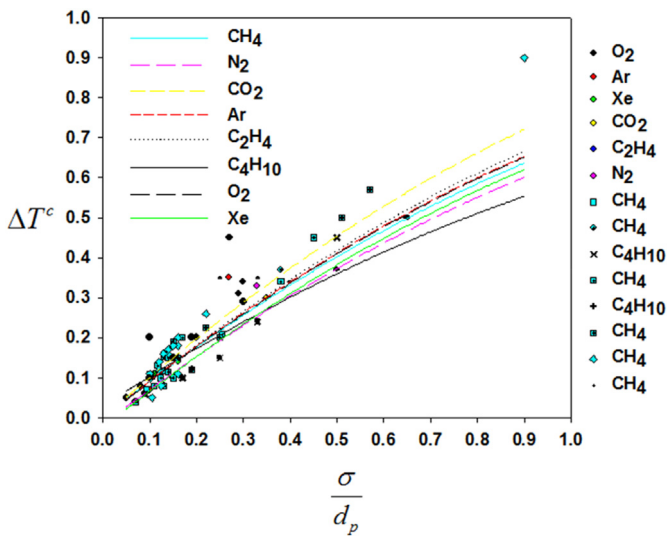


Fig. 4. Critical temperature shifts with respect to pore size. (The symbols and lines represent, respectively, literature data and calculations. References are cited in text.)

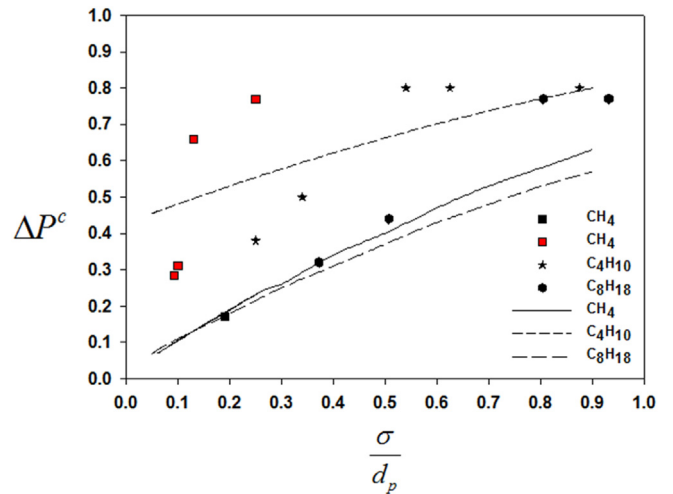


Fig. 5. Critical Pressure shift with respect to pore sizes (symbols and lines represent literature and calculated data, respectively. References are cited in text.).

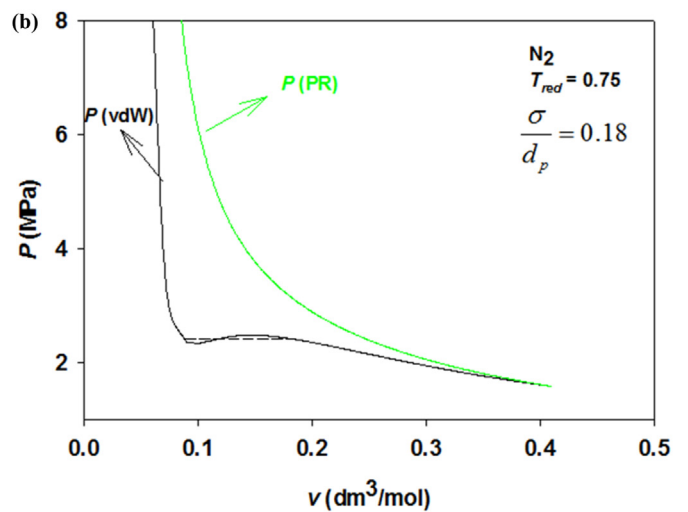
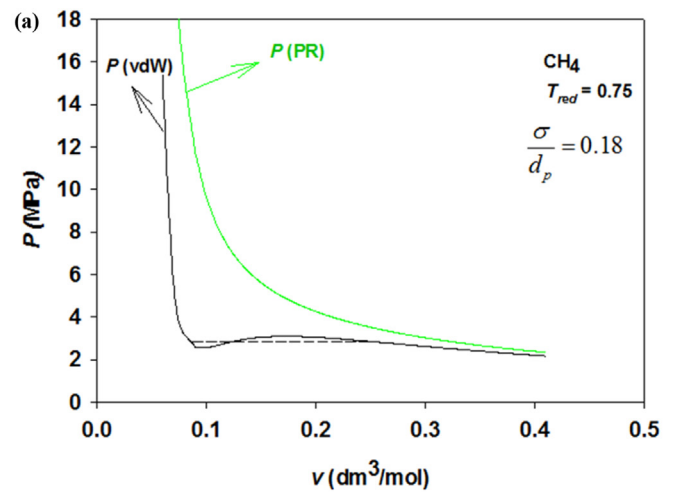


Fig. 6. Confinement effects shown by vdW and PR (dots evidence Maxwell's construction relating to vapor–liquid equilibrium).

Table 1
Calculated critical temperatures and pressures.

Mole	T_c (K)		P_c (bar)	
	Calculated	Ref. (Smith et al., 2005)	Calculated	Ref. (Smith et al., 2005)
CH ₄	191	190.6	46	45.99
C ₂ H ₄	285	282.3	49	50.4
N ₂	126	126.2	34	34

P – v values. In this case a and b are the original PR parameters taken from Peng and Robinson (1976). The results with respect to bulk phase reduced temperature, T_{red} , are presented in Fig. 6. Our calculations clearly render that instead of capillary condensations like in the case of vdW the PR exhibits confinement effects as suppression of fluids into the supercritical states. This means pore proximity effect can result in either vapor–liquid existence, or dense supercritical state as shown by vdW and PR, respectively. We suggest for calculating fluids Pressure-Volume-Temperature (PvT) properties in subcritical or near critical regions first to make sure the possibility of existence of multiphases due to extreme confinement before any sort of predictions, e.g., reserves, transports, etc. by the proposed vdW. The proposed equation can reproduce critical properties of bulk molecules. This indicates the ability of smooth transition from extreme confinement to bulk property. Table 1 shows results of critical temperatures and pressure of three different molecules

$$\left(\begin{array}{l} \sigma \rightarrow 10^{-5}, \quad v = \frac{V}{N} \Big|_{N \rightarrow 6.0123 \times 10^{23}} \\ r_p \rightarrow 10^5 \sigma \end{array} \right).$$

4. Conclusions

A modified form of the vdW EOS is developed to incorporate the effects of nanopore confinements. The model equations not only qualitatively show phase change due to pore proximity but also can quantify critical temperature and pressure shifts by applying Maxwell's equal area rule. The critical temperature shifts follow almost linear relation with pore size reductions up to $\sigma/d_p \approx 0.5$. However in the case of pressures any definite trend cannot be followed. It is noteworthy to mention that the vapor–liquid transitions as observed in Fig. 3 are not necessarily due to the pore proximity only. The calculations are shown for subcritical regions and therefore the VLE may be expected even in bulk phases in addition to having certain confinement effects. As the objective of this study is to predict the pressures exerted by fluid molecules no wall interactions are accounted. This simple model can substitute the expensive laboratory experiments and molecular simulation to deliver answers of phase behavior of fluids in the whole range of pore sizes from the scale of single molecule to free bulk states. The PR (Peng and Robinson, 1976) does not show capillary condensation. However, transforming into supercritical state due to pore proximity is observed. We suggest future extensive investigation on PR to study phase behavior in nanopores.

References

Binder, K., Landau, D., Muller, M., 2003. Monte Carlo studies of wetting, interface localization and capillary condensation. *J. Stat. Phys.* 110, 1411–1514.
Coasne, B., Alba-Simionesco, C., Audonnet, F., Dosseh, G., Gubbins, K., 2009. Adsorption and structure of benzene on silica surfaces and in nanopores. *Langmuir* 25, 10648–10659.
Demontis, P., Strara, G., Suffritti, G., 2003. Behavior of water in the hydrophobic zeolite silicate at different temperatures: a molecular dynamics study. *J. Phys. Chem. B* 107, 4426–4436.
Derouane, E., 2007. On the physical state of molecules in microporous solids. *Microporous Mesoporous Mater.* 104, 46–51.
Devegowda, D., Sapmanee, K., Civan, F., Sigal, R., 2012. Phase behavior of gas

condensates in shale due to pore proximity effects: implications for transport, reserves and well productivity. In: Paper Presented at SPE Annual Technical Conference and Exhibition, San Antonio, TX, USA.
Diaz-Campos, M., 2010. Uncertainties in Shale Gas- in Place Calculations (MS thesis). University of Oklahoma, Norman.
Didar, B., Akkutlu, Y., 2013. Pore-size dependence of fluid phase behavior and properties in organic-rich shale reservoirs. In: Paper Presented at SPE International Symposium on Oilfield Chemistry, The Woodlands, TX, USA.
Dukovski, I., Machta, J., Saravanan, C., Auerbach, S., 2000. Cluster Monte carlo simulations of phase transitions and critical phenomena in zeolites. *J. Chem. Phys.* 113, 3697–3703.
Giaya, A., Thompson, R., 2002. Water confined in cylindrical micropores. *J. Chem. Phys.* 117, 3464–3475.
Giovambattista, N., Rossky, P., Debendetti, P., 2009. Effect of temperature on the structure and phase behavior of water confined by hydrophobic, hydrophilic, and heterogeneous surfaces. *J. Phys. Chem. B* 113, 13723–13734.
Hill, T., 2002. *Thermodynamics of Small Systems*. Courier Dover Publications, New York, pp. 328–329.
Hirschfelder, J., Curtiss, C., Bird, R., 1993. *Molecular Theory of Gases and Liquids*. Wiley, New York, pp. 878–879.
Holt, J., et al., 2006. Fast mass transport through sub-2-nanometer carbon nanotubes. *Science* 312, 1034–1037.
Jana, S., Singh, J., Kwak, K., 2009. Vapor-liquid critical and interfacial properties of square-well fluids in slit pores. *J. Chem. Phys.* 130, 214707.
Jiang, J., Sandler, S., 2005. Adsorption and phase transitions on nanoporous carbonaceous materials: insights from molecular simulations. *Fluid Phase Equilib.* 228, 189–195.
Jiang, J., Sandler, S., 2006. Capillary phase transitions of linear and branched alkanes in carbon nanotubes from molecular simulation. *Langmuir* 22(22), 7391–7399.
Jiang, J., Sandler, S., Schenk, M., Smit, B., 2005. Adsorption and separation of linear and branched alkanes on carbon nanotube bundles from configuration-bias monte carlo simulation. *Phys. Rev. B* 72.
Konno, M., Shibata, K., Saito, S., 1985. Adsorption of light hydrocarbon mixtures on molecular sieving carbon MSC-5A. *J. Chem. Eng. Jpn.* 18, 394–398.
Kotdawala, R., Kazantzis, N., Thompson, R., 2005. Analysis of binary adsorption of polar and nonpolar molecules in narrow slit-pores by mean-field perturbation theory. *J. Chem. Phys.* 123.
McGuiggan, P., Israelachvili, J., 1990. Adhesion and short-range forces between surfaces. Part II: effects of surface lattice mismatch. *J. Mater. Res.* 5, 2232–2243.
Meyra, A., Zarragoicochea, G., Kuz, V., 2005. Thermodynamic equations for a confined fluid at nanometric scale. *Fluid Phase Equilib.* 230, 9–14.
Morishige, K., Shikimi, M., 1998. Adsorption hysteresis and pore critical temperature in a single cylindrical pore. *J. Chem. Phys.* 108.
Morishige, K., Fujii, H., Uga, M., Kinukawa, D., 1997. Capillary critical point of argon, nitrogen, oxygen, ethylene and carbon dioxide in MCM-41. *Langmuir* 13, 3494–3498.
Nicholson, D., Parsonage, N., 1982. Computer Simulation and the Statistical Mechanics of Adsorption. Academic Press, New York, pp. 130–131.
Ortiz, V., Lopez-Alvarez, Y., Lopez, G., 2005. Phase diagrams and capillary condensation of confined in single- and multi-layer nanotube. *Mol. Phys.* 103, 2587–2592.
Peng, D., Robinson, D., 1976. A new two-constant equation of state. *Ind. Eng. Chem. Fundam.* 15, 59–64.
Pot, V., Appert, C., Melayah, A., Rothman, D., Zaleski, S., 1996. Interacting lattice gas automation study of liquid-gas properties in porous media. *J. Phys. II* 6, 1517.
Sakuth, M., Meyer, J., Gmehling, J., 1998. Measurement and prediction of binary adsorption equilibria of vapors on dealuminated Y-zeolite. *Chem. Eng. Process.* 37, 267–277.
Schoen, M., Diestler, D., 1998. Analytical treatment of a simple fluid adsorbed in a slit-pore. *J. Chem. Phys.* 109, 5596–5606.
Severson, B., Snurr, R., 2007. Monte Carlo simulation of n-alkane adsorption isotherms in carbon slit pores. *J. Chem. Phys.* 126.
Singer, I., Pollock, H., 1992. In: *Fundamentals of Friction: Macroscopic and Microscopic Processes*. Nato Science Series E. Springer, Netherlands, pp. 350–351.
Singh, S., Sinha, A., Deo, G., Singh, J., 2009. Vapor-liquid phase coexistence, critical properties, and surface tension of confined alkanes. *J. Phys. Chem.* 113, 7170–7180.
Smith, J., Van Ness, H., Abbott, M., 2005. *Introduction to Chemical Engineering Thermodynamics*, seventh ed. McGraw Hill Chemical Engineering Series, New York, pp. 548–549.

- Travalloni, L., Castier, M., Tavares, F., Sandler, S., 2010. Critical behavior of pure fluids from an extension of the van der Waals equation of state. *J. Supercrit. Fluids* 55, 455–461.
- Travalloni, L., Castier, M., Tavares, F., Sandler, S., 2010. Thermodynamic modeling of confined fluids using an extension of the generalised van der Waals theory. *Chem. Eng. Sci.* 65, 3088–3099.
- Tsallis, C., 1988. Possible generalization of Boltzmann-Gibbs statistics. *J. Stat. Phys.* 52, 479–487.
- Tsallis, C., 1999. Nonextensive statistics: theoretical, experimental and computational evidence and connections. *Braz. J. Phys.* 29, 1–35.
- Vakili-Nezhaad, G., Mansoori, G., 2004. An application of non-extensive statistical mechanics to nanosystems. *J. Comput. Theor. Nanosci.* 1, 227–229.
- Vakili-Nezhaad, G., Mansoori, G., 2006. Thermodynamic interpretation of the fragmentation phenomenon in nanopores. *Asian J. Chem.* 18, 2398–2400.
- Varnik, F., Baschnagel, J., Binder, K., 2000. Molecular dynamics results on the pressure tensor of polymer films. *J. Chem. Phys.* 113, 4444.
- Vishnyakov, A., Piotrovskaya, E., Brodskaya, E., Votyakov, E., Tovbin, Y., 2001. Critical properties of Lennard-Jones fluids in narrow slit pores. *Langmuir* 17, 4451–4458.
- Weast, R.C., 1972. *Handbook of Chemistry and Physics*, 53rd ed. Chemical Rubber Company, Cleveland, pp. 1430–1431.
- Wu, J., 2006. Density functional theory for chemical engineering: from capillary to soft materials. *AIChE J.* 52, 1169–1193.
- Yun, J., Durren, T., Keil, F., Seaton, N., 2004. Adsorption of methane, ethane, and their binary mixtures on MCM-41: experimental evaluation of methods for the prediction of adsorption equilibrium. *Langmuir* 18, 2693–2701.
- Zarragoicoechea, G., Kuz, V., 2002. van der Waals equation of state for a fluid in a nanopore. *Phys. Rev. E* 65, 021110.
- Zarragoicoechea, G., Kuz, V., 2004. Critical shift of a confined fluid in a nanopore. *Fluid Phase Equilib.* 220, 7–9.